

Field-induced control of ferrofluid emulsion rheology and droplet break-up in shear flows

Lucas H. P. Cunha,^{1,2, a)} Ivan R. Siqueira,^{2, b)} Taygoara F. Oliveira,^{1, c)} and Hector D. Ceniceros^{3, d)}

¹⁾*Department of Mechanical Engineering, Universidade de Brasília, Brasília, DF 70910-900, Brazil*

²⁾*Department of Chemical and Biomolecular Engineering, Rice University, Houston, TX 77005, USA*

³⁾*Department of Mathematics, University of California Santa Barbara, Santa Barbara, CA 93106, USA*

(Dated: 28 November 2018)

Ferrofluid droplets have been widely used in a number of cutting-edge applications in microfluidics, biomedicine, and microrheology. In many cases, the droplet is simultaneously subjected to a hydrodynamic flow and an external magnetic field. However, the response of a ferrofluid droplet under these forces in terms of deformation, inclination, and potential break-up into smaller droplets is not yet fully understood. In this work, we present a numerical study of the dynamics of a two-dimensional ferrofluid droplet suspended in a non-magnetic, immiscible liquid when the two-phase fluid undergoes a simple shear flow under the action of an external, uniform magnetic field. The model consists of the magnetostatic Maxwell's equations and the incompressible Navier-Stokes equations with additional terms that take into account both magnetic and capillary forces on the droplet. The resulting system of fully coupled, non-linear equations is accurately solved with the Projection Method together with the Level Set Method to capture the droplet interface. Our results show that the external magnetic field strongly affects the droplet deformation and inclination relative to the flow. We investigate the effects of the external field-induced droplet distortion on the viscosity of the resulting complex fluid when the two-phase liquid is viewed as a dilute emulsion of ferrofluid droplets. Notably, the viscosity of the ferrofluid emulsion can be either dramatically increased or decreased depending on the intensity and direction of the external magnetic field. We also analyze for the first time the effects of the external magnetic field on the break-up process of ferrofluid droplets undergoing large deformations. Remarkably, the external magnetic field can be adjusted to control the droplet break-up process both in terms of time to break-up and size of satellite droplets. These new insights indicate the potential of external magnetic fields as tunable tools to control the rheology of ferrofluid emulsions and topology of ferrofluid droplets in shear flows.

^{a)}E-mail: lh36@rice.edu;

^{b)}E-mail: irs@rice.edu

^{c)}E-mail: taygoara@unb.br

^{d)}E-mail: hdc@math.ucsb.edu

I. INTRODUCTION

Ferrofluid emulsions are two-phase mixtures consisting of ferrofluid droplets suspended in a non-magnetic, immiscible liquid. Their macroscopic behavior is dictated by complex physical phenomena that occur at the microscopic level, such as droplet deformation, rotation, and break-up, which, in turn, are ruled by the combined action of hydrodynamic and magnetic effects. As a consequence, suspensions of ferrofluid droplets are complex fluids whose response under flow can be controlled by external magnetic fields. As recently reviewed by Torres-Díaz and Rinaldi¹, there is a wide range of applications supporting the growing research on the behavior of ferrofluid droplets as magnetically controllable fluids. For instance, their interaction with external magnetic fields have been extensively explored in microfluidics^{2,3} and biomedical processes, such as targeted drug delivery⁴⁻⁶ and restorative treatment of retinal detachment⁷⁻⁹. Recently, new microrheology techniques based on the field-induced motion of an immersed ferrofluid droplet have been proposed for measuring the viscosity and surface tension of liquids^{10,11}. Thus, a fundamental understanding of the behavior of ferrofluid droplets under the combined action of hydrodynamic flows and external magnetic fields is essential for improving existing applications and developing new technologies.

Since the pioneering works of Sherwood¹² and Séro-Guillaume, Zouaoui, Bernardin, and Brancher¹³, the response of ferrofluid droplets to external magnetic fields has been substantially investigated. Fundamental studies on the equilibrium shape of ferrofluid droplets under applied fields¹⁴⁻¹⁸ and on the field-induced motion of ferrofluid droplets suspended in non-magnetic liquids¹⁹⁻²¹ abound. It has also been shown that external magnetic fields play an important role on formation and break-up of ferrofluid droplets in microfluidic systems²²⁻²⁶, viscous fingering phenomena in Hele-Shaw cells^{27,28}, self-assembly of ferrofluid droplets into ordered structures²⁹, and spreading of ferrofluid droplets^{30,31}.

Notwithstanding, most of the research to date has centered on the interaction of ferrofluid droplets and magnetic fields in a quiescent flow. One exception is the recent numerical work presented by Jesus, Roma, and Ceniceros³² on the dynamics of a three-dimensional ferrofluid droplet in shear flows under external magnetic fields. However, due to the high computational cost of the simulations, the authors did not address large droplet deformations and break-up conditions. Other works that deserve special attention are the ones presented

by Hassan, Zhang, and Wang³³ and Capobianchi, Lappa, and Oliveira³⁴, which focused on the deformation, inclination, lateral migration and transient relaxation of ferrofluid droplets in simple shear flows under the influence of external magnetic fields. However, the effects of the external field on the viscosity of the resulting ferrofluid emulsion and droplet break-up process due to large deformations were not explored either.

In this work, we present a detailed numerical study on the response of a two-dimensional ferrofluid droplet suspended in a non-magnetic, immiscible liquid when the system undergoes the combined action of a simple shear flow and an external, uniform magnetic field. We are able to explore large deformations and droplet break-up by employing a highly accurate interface capturing method to compute the topological changes of the droplet surface when the rupture occurs. The mathematical modeling couples the magnetostatic Maxwell's equations and the incompressible Navier-Stokes equations with additional terms related to magnetic and capillary forces. The model is solved with the Project Method together with the Level Set method to capture the dynamics of the droplet interface. Our results indicate that the magnetic field can drastically affect the droplet deformation and inclination in the flow, which, in turn, play a key role in the effective viscosity of the resulting dilute emulsion of ferrofluid droplets. We also show that the intensity and direction of the external magnetic field can be adjusted to control the droplet break-up process both in terms of break-up time and size of the satellite droplet.

The remainder of this article is organized as follows. In Section II, we present the mathematical modeling of the problem, including the governing equations and dimensionless parameters. Section III summarizes the numerical methodology used in the simulations. The numerical results are presented and discussed in Section IV, and some concluding remarks are given in Section V. Further details of the numerical resolution are given in Appendix A.

II. MATHEMATICAL MODEL

A. Problem formulation

Consider a channel between two parallel plates filled with a non-magnetizable liquid in which there is a suspended, neutrally buoyant, ferrofluid droplet. The continuous phase has viscosity η and magnetic permeability μ_0 , which is assumed to be equal to the magnetic

permeability of the free space (that is, $\mu_0 = 4\pi \times 10^{-7} \text{ H}\cdot\text{m}^{-1}$). The ferrofluid droplet, which is initially circular with radius a and centered at the channel center, has viscosity $\lambda\eta$ and magnetic permeability $\zeta\mu_0$. Both phases are assumed to be Newtonian and incompressible, and the two-phase fluid can be seen as a dilute emulsion of ferrofluid drops. The system is subjected to a simple shear flow with shear rate $\dot{\gamma}$ caused by the movement of the channel walls in opposite directions. Notice that the flow is symmetric with respect to the droplet initial position and the velocity along the channel centerline is zero. Furthermore, the system is also subjected to an external, uniform external magnetic field \mathbf{H}_0 that can be either parallel or perpendicular to the main flow direction (that is, the x -direction). Figure 1 shows a sketch of the problem in which the external magnetic field is parallel to the flow direction; the ferrofluid droplet is confined in the region Ω_i (bounded by Γ_i) and the continuous phase occupies the region Ω_o (bounded by Γ_o).

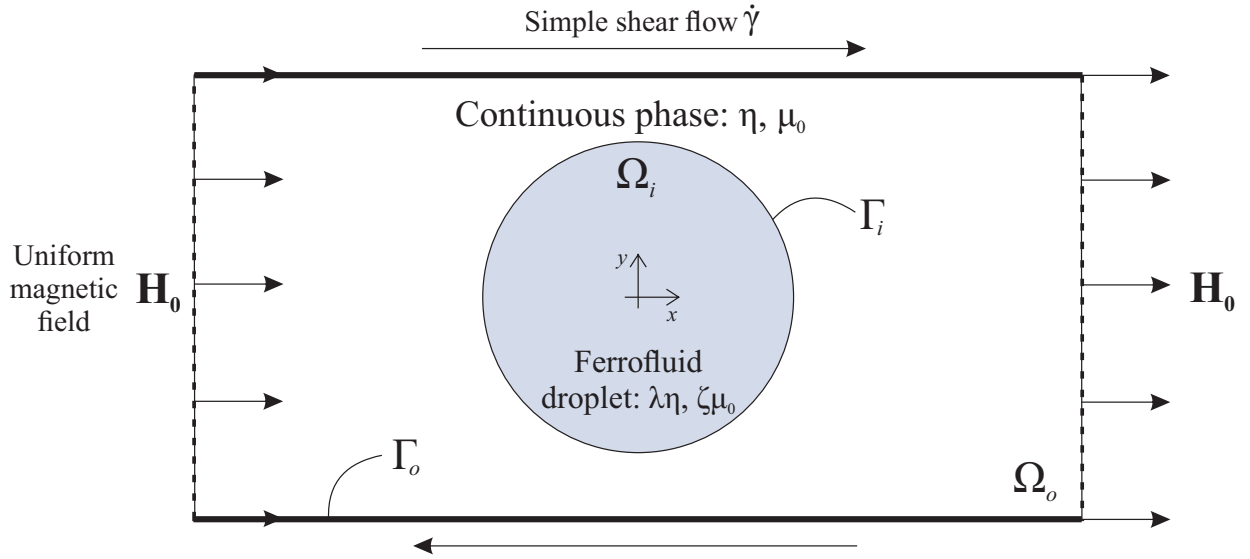


FIG. 1. Sketch of the problem (not to scale).

B. Governing equations for the magnetic and hydrodynamic problems

The applied magnetic field affects the magnetization \mathbf{M} of the ferrofluid, which, in turn, contributes to the magnetic induction as $\mathbf{B} = \mu_0(\mathbf{H} + \mathbf{M})$, where \mathbf{H} is the magnetic field. In the absence of electric currents, \mathbf{H} and \mathbf{B} satisfy the magnetostatic Maxwell's equations:

$\nabla \cdot \mathbf{B} = 0$ and $\nabla \times \mathbf{H} = \mathbf{0}$. We further assume that the ferrofluid is superparamagnetic, such that $\mathbf{M} = \chi \mathbf{H}$, where χ is the magnetic susceptibility. This assumption leads to $\mathbf{B} = \mu_0 \zeta \mathbf{H}$, where $\mu_0 \zeta = \mu_0(1 + \chi)$ is the magnetic permeability of the dispersed ferrofluid phase. Since \mathbf{H} is an irrotational field, there is a scalar potential ψ that satisfies $\mathbf{H} = -\nabla \psi$. Then, the magnetic problem is reduced to

$$\nabla \cdot (\mu_0 \zeta(\mathbf{x}) \nabla \psi) = 0, \quad (1)$$

where \mathbf{x} is the position vector. In Eq. (1), the permeability ratio $\zeta = \zeta(\mathbf{x})$ is extended to the entire fluid domain, being equal to the unit for the continuous phase.

The two-phase fluid flow is governed by the incompressible Navier-Stokes equations, as follows,

$$\nabla \cdot \mathbf{u} = 0, \quad (2)$$

$$\rho \frac{D\mathbf{u}}{Dt} = -\nabla p + \nabla \cdot [\lambda(\mathbf{x})\eta (\nabla \mathbf{u} + \nabla \mathbf{u}^T)] + \mathbf{F}_m + \mathbf{F}_s, \quad (3)$$

where \mathbf{u} is the velocity field, ρ is the density, t is the time, p is the pressure field, \mathbf{F}_m is the magnetic force (density) on the ferrofluid phase, and \mathbf{F}_s is the capillary force (density) on the droplet interface. Notice that viscosity ratio $\lambda = \lambda(\mathbf{x})$ is also extended to the entire domain, being equal to one for the continuous phase. The magnetic force is given by³⁵ $\mathbf{F}_m = \mu_0 \mathbf{M} \cdot \nabla \mathbf{H} = \mu_0 (\zeta(\mathbf{x}) - 1) \mathbf{H} \cdot \nabla \mathbf{H}$, and the capillary force is defined as $\mathbf{F}_s = -\sigma \kappa \delta_s \mathbf{n}$, where σ is the interfacial tension, κ is the curvature, δ_s is a Dirac delta distribution on the liquid-liquid interface, and \mathbf{n} is the unit normal vector outward the droplet surface. Notice that the interaction between the droplet and the basis liquid is purely hydrodynamic, that is, except for capillary effects, there is no additional stress induced by the ferrofluid phase in the absence of an external magnetic field.

We non-dimensionalize the governing equations by using the following dimensionless variables: $\mathbf{u}^* = \mathbf{u}/\dot{\gamma}a$, $t^* = t\dot{\gamma}$, $\mathbf{x}^* = \mathbf{x}/a$, $p^* = p/(\rho a^2 \dot{\gamma}^2)$, and $\mathbf{H}^* = \mathbf{H}/\|\mathbf{H}_0\|$. Dropping the superscript $*$ to alleviate the notation, the dimensionless form of Eqs. (2) and (3) becomes

$$\nabla \cdot \mathbf{u} = 0, \quad (4)$$

$$\begin{aligned} \frac{D\mathbf{u}}{Dt} = & -\nabla p + \frac{1}{Re} \nabla \cdot [\lambda(\mathbf{x}) (\nabla \mathbf{u} + \nabla \mathbf{u}^T)] + \frac{Ca_{mag}}{Ca Re} (\zeta(\mathbf{x}) - 1) \mathbf{H} \cdot \nabla \mathbf{H} \\ & - \frac{1}{Ca Re} \kappa \delta_s \mathbf{n}. \end{aligned} \quad (5)$$

Three dimensionless numbers appear in the formulation: (i) the Reynolds number, $Re = \rho \dot{\gamma} a^2 / \eta$, which represents the ratio of inertial to viscous forces; (ii) the capillary number, $Ca = \eta a \dot{\gamma} / \sigma$, which denotes the ratio of viscous to capillary forces; and (iii) the magnetic capillary number, $Ca_{mag} = \mu_0 a \|\mathbf{H}_0\|^2 / \sigma$, which represents the ratio of magnetic to capillary forces. Notice that the magnetic capillary number plays the same role as the magnetic Bond number recently used by Jesus *et al.*³² and Hassan *et al.*³³ to study the dynamics of ferrofluid droplets in shear flows under external magnetic fields. These three dimensionless groups together with the viscosity and magnetic permeability ratios, λ and ζ , respectively, are the main parameters of the model. For the reader interested in typical dimension values for the fluid properties, external field intensity, and droplet size used in experiments and practical applications, we suggest the review by Torres-Díaz and Rinaldi¹ and references therein.

Boundary conditions are needed to solve Eqs. (1), (4) and (5), as follows: (i) for the magnetic potential field, we impose a constant flux condition at the four boundaries to obtain an external, uniform magnetic field; notice that these fluxes can be zero or not depending on the direction of the external field, which can be either parallel or perpendicular to the main flow direction; (ii) for the velocity field, we consider the no-slip condition at the channel walls together with periodic boundary conditions in the flow direction; and (iii) for the pressure field, we apply the no-flux condition at the channel walls and periodic boundary conditions in the flow direction.

Finally, it is worth mentioning that the two-phase system can be seen as a dilute emulsion of ferrofluid droplets. To analyze the effect of the external magnetic field on the emulsion rheology, we consider the emulsion reduced viscosity, which is defined as³⁶

$$[\eta] = \frac{\langle \sigma_{xy} \rangle - \eta \dot{\gamma}}{\eta \dot{\gamma} \beta}, \quad (6)$$

where $\langle \sigma_{xy} \rangle$ is the volume-averaged shear stress on the moving walls and β is the volume fraction of the dispersed phase.

C. Level set formulation for droplet dynamics

Since the droplet shape, position, and even topology change in time, we are dealing with a free-boundary problem. Here, we capture the droplet dynamics with the Level Set method³⁷. The interface between the liquids is represented at all times as the zero-level set of a scalar-valued function $\phi(\mathbf{x}, t)$, such that, for each time t , the droplet surface is the set of points \mathbf{x} such that $\phi(\mathbf{x}, t) = 0$. The level set function is advected by the flow field according to

$$\frac{\partial \phi}{\partial t} + \mathbf{u} \cdot \nabla \phi = 0. \quad (7)$$

The level set function also serves as an indicator or maker function to evaluate the piecewise constant $\lambda(\mathbf{x})$ and $\zeta(\mathbf{x})$, such that the discontinuities across the liquid-liquid interface are replaced by smooth transitions occurring in a thin region of size ε . To this end, we consider a mollified Heaviside function defined as

$$H_\varepsilon(\phi) = \begin{cases} 0, & \text{if } \phi < -\varepsilon, \\ \frac{1}{2} \left[1 + \frac{\phi}{\varepsilon} + \frac{1}{\pi} \sin \left(\frac{\pi \phi}{\varepsilon} \right) \right], & \text{if } |\phi| \leq \varepsilon, \\ 1, & \text{if } \phi > \varepsilon. \end{cases} \quad (8)$$

The piecewise constant $\lambda(\mathbf{x})$ and $\zeta(\mathbf{x})$ are then replaced by the smooth functions $\lambda_\varepsilon(\phi) = \lambda + (1 - \lambda)H_\varepsilon(\phi)$ and $\zeta_\varepsilon(\phi) = \zeta + (1 - \zeta)H_\varepsilon(\phi)$. The level set function is also used to define a mollified Dirac delta distribution,

$$\delta_\varepsilon(\phi) = \frac{\partial H_\varepsilon(\phi)}{\partial \phi} = \begin{cases} 0, & \text{if } |\phi| > \varepsilon, \\ \frac{1}{2\varepsilon} \left[1 + \cos \left(\frac{\pi \phi}{\varepsilon} \right) \right], & \text{if } |\phi| \leq \varepsilon, \end{cases} \quad (9)$$

as well as the unit normal vector outward the droplet surface, $\mathbf{n} = \nabla \phi / |\nabla \phi|$, and the droplet curvature, $\kappa = \nabla \cdot (\nabla \phi / |\nabla \phi|)$. Those definitions are then used to couple the magnetic and hydrodynamic governing equations with the level set function, leading to a model valid throughout the entire domain of the two-phase fluid flow.

III. NUMERICAL METHODOLOGY

A. Numerical scheme

The numerical methodology employed in this work consists of three main components: (i) a second-order method for the elliptic problem governing the magnetic potential field, ψ ; (ii) a second-order non-stiff Projection Method for the hydrodynamic problem governing the velocity and pressure fields, \mathbf{u} and p ; and (iii) a high-order Total Variation Diminishing (TVD) scheme to advance the level set function, ϕ . A uniform staggered grid is used for the discretization of the problem domain.

A standard second-order finite difference is used for the spatial discretization of Eqs. (1), (4), and (5). The elliptic problem for the magnetic potential field is solved efficiently with a preconditioned Conjugate Gradient Method. The fluid flow problem is solved with a splitting Projection Method³⁸ with the semi-implicit modification introduced by Badalassi, Cenicerros, and Banerjee³⁹, such that

$$\frac{3\mathbf{u}^* - 4\mathbf{u}^n + \mathbf{u}^{n-1}}{2\Delta t} = \frac{\bar{\lambda}}{Re} \nabla^2 \mathbf{u}^* + \mathcal{G}(\hat{\mathbf{u}}, \phi^n, \mathbf{H}^n) + \mathbf{F}_s(\phi^n), \quad (10)$$

$$\frac{3}{2\Delta t} (\mathbf{u}^{n+1} - \mathbf{u}^*) = -\nabla p^{n+1}, \quad (11)$$

where

$$\begin{aligned} \mathcal{G}(\hat{\mathbf{u}}, \phi^n, \mathbf{H}^n) &= -\hat{\mathbf{u}} \cdot \nabla \hat{\mathbf{u}} - \frac{\bar{\lambda}}{Re} \nabla^2 \hat{\mathbf{u}} + \frac{1}{Re} \nabla \cdot \left(\lambda_\varepsilon(\phi^n) (\nabla \hat{\mathbf{u}} + \nabla \hat{\mathbf{u}}^T) \right) \\ &\quad + \frac{Ca_{mag}}{Ca Re} (\zeta_\varepsilon(\phi^n) - 1) \mathbf{H}^n \cdot \nabla \mathbf{H}^n, \end{aligned} \quad (12)$$

$$\mathbf{F}_s(\phi^n) = -\frac{1}{Ca Re} \nabla \cdot \left(\frac{\nabla \phi^n}{|\nabla \phi^n|} \right) \delta_\varepsilon(\phi^n) \frac{\nabla \phi^n}{|\nabla \phi^n|}, \quad (13)$$

$\bar{\lambda} = \max\{1, \lambda_\varepsilon(\phi^n)\}$, and $\hat{\mathbf{u}} = 2\mathbf{u}^n - \mathbf{u}^{n-1}$. The pressure p^{n+1} is then obtained by solving $\nabla^2 p^{n+1} = \frac{3}{2\Delta t} \nabla \cdot \mathbf{u}^*$.

Finally, the advection of the level set function given in Eq. (7) is integrated with a combined third-order TVD Runge-Kutta method for the temporal discretization and a fifth-order Weighted Essentially Non-Oscillator (WENO) scheme for the computation of the spatial derivative⁴⁰. The level set function is initialized as a signed distance to the droplet surface. However, a well-known difficulty associated to the Level Set Method is the progressive

distortion of the level set function as the problem evolves. Because not all fluid particles move with the same velocity as the interface velocity, after some time $\phi(\mathbf{x}, t)$ no longer represents a signed distance function to the droplet surface, i.e. $|\nabla\phi| \neq 1$, which leads to inaccurate representations of the droplet interface and its associated geometric quantities (e.g. normal and tangent vectors and curvature)^{41,42}. To overcome this issue, we employ the reinitialization method of Sussman, Smereka, and Osher⁴³.

In all simulations, we set $\varepsilon = 1.5h$ for the interfacial thickness, where h is the mesh size. The time step is chosen to satisfy the condition $\Delta t = 0.05h/\sqrt{2(f_{cm} + f_{cc})}$, where $f_{cm} = Ca_{mag}(\zeta - 1)/Ca Re$ is a characteristic magnetic force and $f_{cc} = 1/Ca Re$ is a characteristic capillary force. A mesh convergence test for the overall numerical scheme is presented in Appendix A.

Formally, the overall method is second order accurate in space and time but due to the regularization of discontinuous material quantities (effectively a diffuse interface approach) the accuracy near the interface is expected to be only first order.

B. Validation

We first validate the model and numerical methodology with two benchmark problems. First, we consider the deformation of a ferrofluid droplet under an external, uniform magnetic field in a quiescent flow. The droplet equilibrium shape, which is approximately ellipsoidal, is dictated by a balance between magnetic and capillary forces. The experiments of Flament, Lacis, Bacri, Cebers, Neveu, and Perzynski¹⁴ in a Hele-Shaw cell provide an appropriate set of data for comparison with our two-dimensional numerical predictions. We use $\lambda = 1$ and $\zeta = 3.2$ in a 12×12 square domain discretized with 256×256 cells. Figure 2 shows a comparison of the experimental results of Flament *et al.*¹⁴ with our numerical predictions for the equilibrium droplet form factor e , defined here as the ratio of the length of minor and major axes, respectively, as a function of Ca_{mag} . As can be observed in this figure, there is an excellent agreement for the general physical trend. We see an average deviation of only 4.66% for the full range of Ca_{mag} explored here. This small difference might be due to experimental factors and/or to the two-dimensional assumption of the Hele-Shaw cell flow. Note the droplet equilibrium shape is also well predicted by the numerical simulations, as Fig. 3 displays.

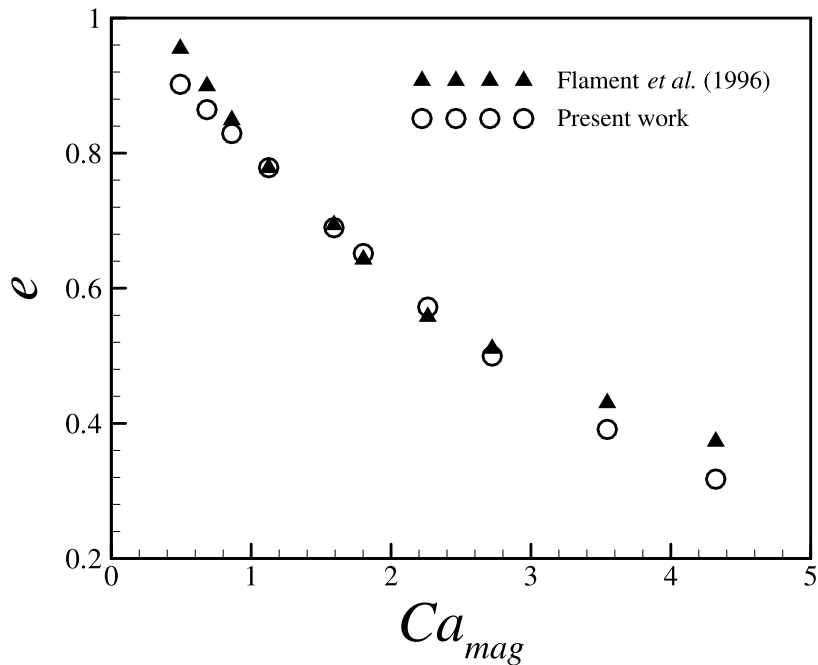


FIG. 2. Comparison with the experimental results of Flament *et al.*¹⁴ for the droplet equilibrium form factor, e , as a function of magnetic capillary number, Ca_{mag} . Simulations performed with $\lambda = 1$ and $\zeta = 3.2$.

Second, we consider a droplet undergoing a simple shear flow in the absence of an external magnetic field. We have compared our numerical results with those of Ghigliotti, Biben, and Misbah⁴⁴, who analyzed a similar problem using a phase field (PF) model under Stokes flow regime (that is, $Re = 0$). The shear flow deforms and rotates the droplet, such that its equilibrium shape is usually not spherical and not aligned with the flow direction. Figure 4 shows the droplet inclination angle relative to the main flow direction, θ , and the emulsion reduced viscosity, $[\eta]$, as functions of the viscosity ratio, λ , for $Re = 0.01$ and $Ca = 0.3$. Although we see a good qualitative agreement between our predictions and those of Ghigliotti *et al.*⁴⁴, there is a relative difference of 4.8% for the reduced viscosity and about 2.2% for the inclination angle. This quantitative discrepancy can be attributed to inertial effects – our simulations were performed with $Re = 0.01$ and the PF model of Ghigliotti *et al.*⁴⁴ is for $Re = 0$ – and, more importantly, to the dependence of the capillary number on the interface thickness in the PF model⁴⁵. Despite these model differences, we note that there is a good agreement in the droplet equilibrium shape, as Fig. 5 demonstrates for $\lambda = 2$.

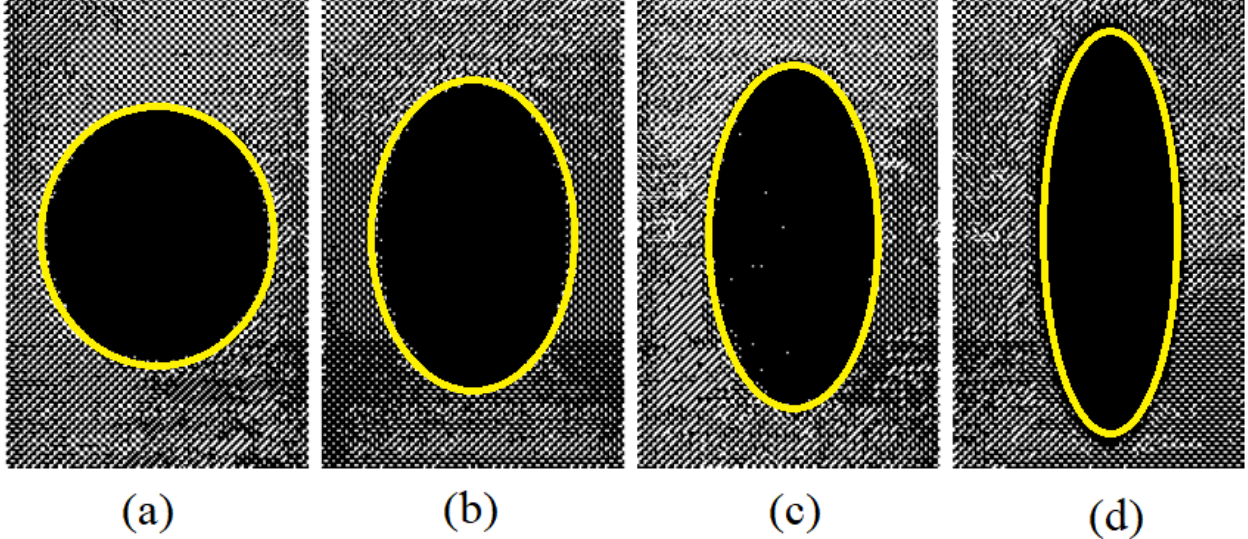


FIG. 3. Comparison of the ferrofluid droplet equilibrium shape obtained experimentally by Flament *et al.*¹⁴ (black and white background) and our numerical predictions (yellow contour) for (a) $Ca_{mag} = 0.5$, (b) $Ca_{mag} = 1.8$, (c) $Ca_{mag} = 2.7$, and (d) $Ca_{mag} = 4.3$. Simulations performed with $\lambda = 1$ and $\zeta = 3.2$.

IV. RESULTS AND DISCUSSIONS

A. Droplet inclination and ferrofluid emulsion viscosity under external magnetic fields

As recently elucidated by Jesus *et al.*³² and Hassan *et al.*³³, external magnetic fields can significantly affect the deformation and inclination of ferrofluid droplets in shear flows. This, in turn, has a direct effect on the reduced viscosity of the two-phase fluid when it is seen as a dilute emulsion of ferrofluid droplets. Here, we analyze this phenomenon using the following procedure. First, we compute the steady state response of a ferrofluid droplet under shear in the absence of an external magnetic field. Then, we turn on the magnetic field and compute the new droplet equilibrium shape and the corresponding reduced viscosity. In this study, we fix $Re = 0.01$, $Ca = 0.1$, $\lambda = 2$, $\zeta = 2$, and consider external magnetic fields parallel and perpendicular to the main flow direction. With no applied field, $2\theta/\pi = 0.41$, $[\eta] = 1.66$, and the droplet does not break. All simulations were performed in a 12×12 square domain discretized with 400×400 cells.

Figure 6 shows the droplet inclination and reduced viscosity as functions of the external

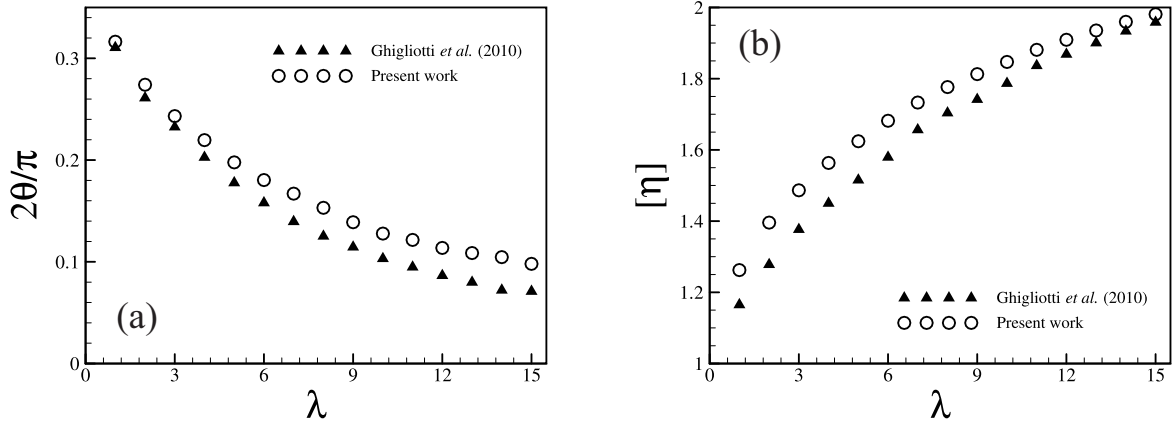


FIG. 4. Comparison with the phase field results of Ghigliotti *et al.*⁴⁴ for (a) droplet inclination, θ , and (b) reduced viscosity, $[\eta]$, as functions of the viscosity ratio, λ . Simulations performed with $Re = 0.01$ and $Ca = 0.3$.

field intensity (expressed in terms of Ca_{mag}). As the field intensity increases, the droplet major axis tends to become more aligned with the external field direction. Thus, when the external magnetic field is parallel to the flow direction, θ decreases with Ca_{mag} and tends asymptotically to zero for sufficiently large Ca_{mag} . As the droplet gets more aligned with the flow, the streamlines get less distorted around the droplet surface, as Fig. 7(a) shows. As a consequence, $[\eta]$ decreases with Ca_{mag} . For instance, at $Ca_{mag} = 20$, $[\eta] = 0.62$, which represents a decrease of 63% relative to the case where there is no applied field, and the inclination is $2\theta/\pi = 0.002$. On the other hand, when the external field is perpendicular to the flow direction, θ increases with Ca_{mag} , as expected. However, as the field induces a droplet deformation in the vertical direction, it increases the shear effects which tend to rotate the droplet back to the extensional quadrant of shear. The final droplet equilibrium shape depends critically on this competition between field-induced stretching and shear stress. The misalignment of the droplet with the flow requires that the streamlines deflect significantly to conform to the droplet shape, as shown in Fig. 7(b), which leads to a higher reduced viscosity. Therefore, $[\eta]$ strongly increases with Ca_{mag} when the applied field is perpendicular to the flow. At $Ca_{mag} = 20$, $[\eta] = 9.04$, which represents an increase of almost one order of magnitude with respect to the zero-field case, and $2\theta/\pi = 0.91$. Figure 8 shows the droplet equilibrium shape for different values of Ca_{mag} when the external field

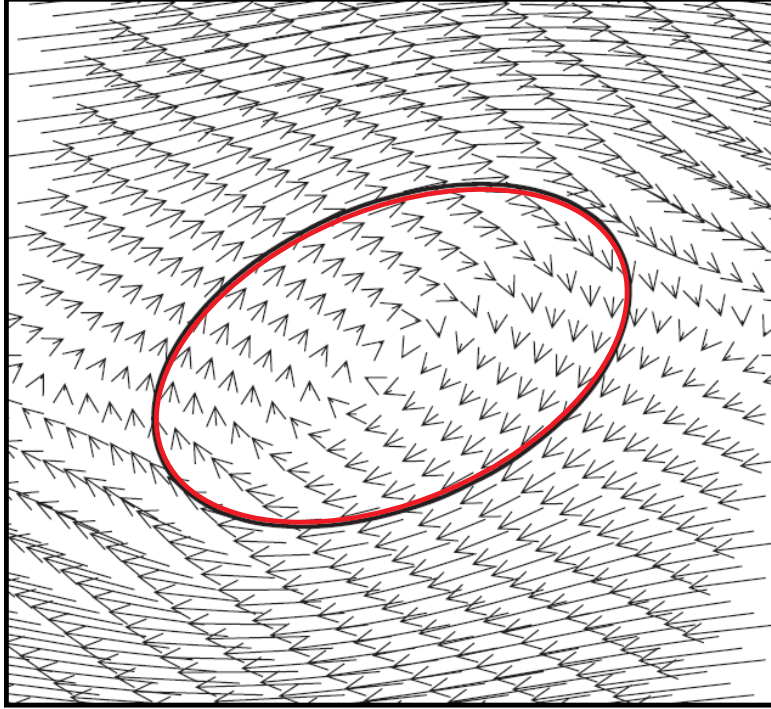


FIG. 5. Comparison of the ferrofluid droplet equilibrium shape obtained with the Stokes-PF model of Ghigliotti *et al.*⁴⁴ (black and white background with the velocity field) and our numerical predictions (red contour). Simulations performed with $Re = 0.01$, $Ca = 0.3$, and $\lambda = 2$.

is parallel and perpendicular to the flow direction.

B. Field-induced control of droplet break-up

External force fields offer the possibility to control emulsion rheology in shear flows by inducing or hindering topological changes in the suspended droplets. Recent works have investigated this effect for emulsions in which the droplets undergo small deformations under external electrical fields^{46–48}. Here, we focus on the effects of external magnetic fields on the rupture of a ferrofluid droplet in shear flows and do not restrict our study to small deformations.

First, we consider a case where the sheared droplet breaks-up in the absence of an external magnetic field (that is, $Ca_{mag} = 0$) and examine how an external field, parallel or perpendicular to the flow direction, affects the rupture. We take $Re = 1$, $Ca = 0.5$, $\lambda = 1.2$,

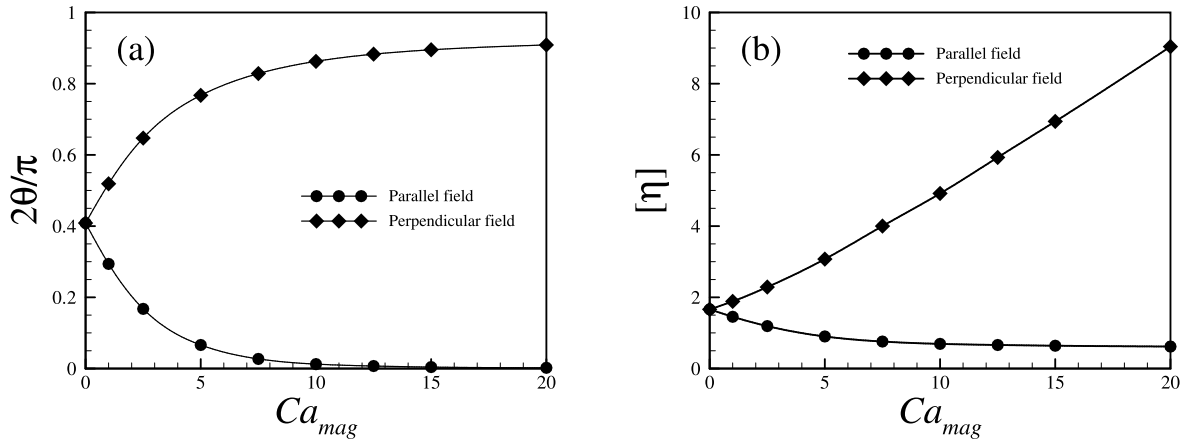


FIG. 6. Effects of the external magnetic field on the (a) droplet inclination, θ , and (b) reduced viscosity, $[\eta]$, as a function of the magnetic capillary number, Ca_{mag} . Simulations performed with $Re = 0.01$, $Ca = 0.1$, $\lambda = 2$, and $\zeta = 2$.

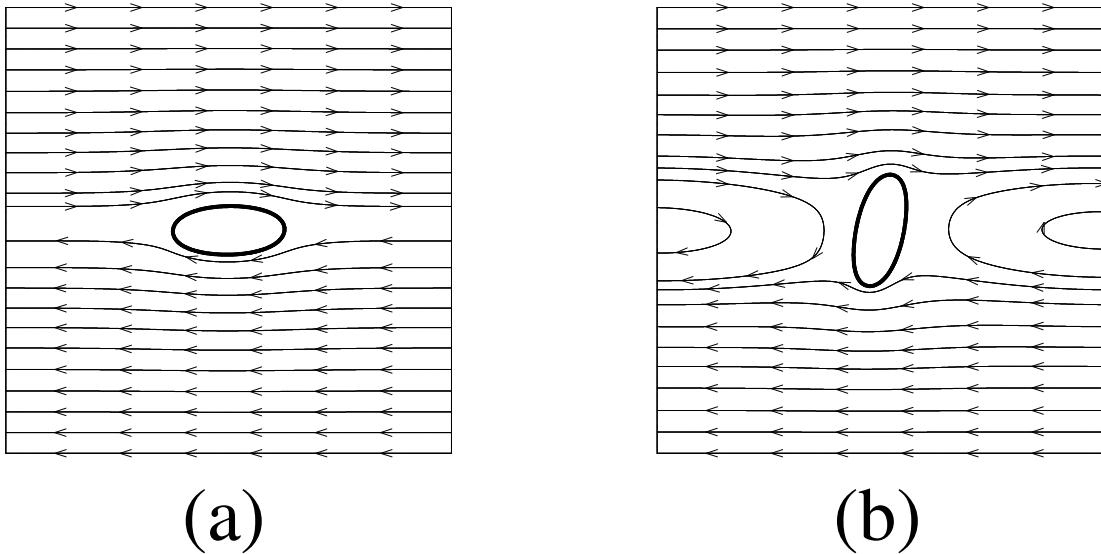


FIG. 7. Streamlines of the flow for $Ca_{mag} = 10$ when the external magnetic field is (a) parallel and (b) perpendicular to the flow direction.

and $\zeta = 2$ for this study. The channel is a 12×6 rectangle discretized with 300×150 cells. Figure 9 shows snapshots of the droplet deformation and its eventual rupture into three smaller, daughter droplets. The smallest daughter droplet is usually referred to as satellite droplet, being very common in droplet break-up process.

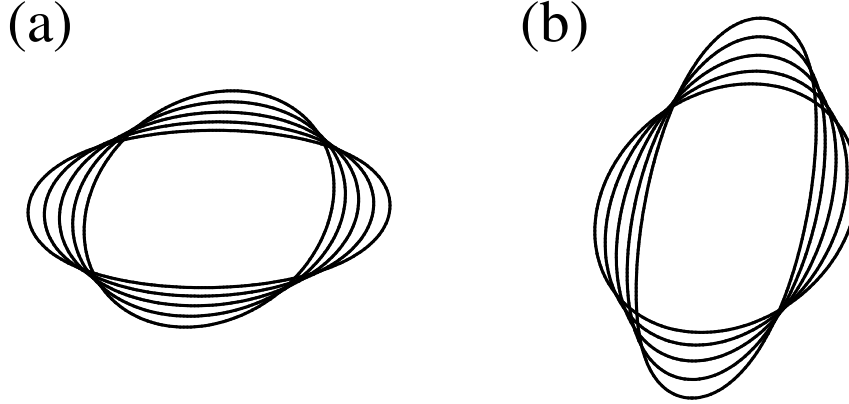


FIG. 8. Droplet equilibrium shape for $Ca_{mag} = 0, 2.5, 5, 7.5,$ and 10 when the external magnetic field is (a) parallel and (b) perpendicular to the flow direction.

We first analyze the effect of an external magnetic field parallel to the flow direction. Snapshots of the droplet evolution for $Ca_{mag} = 2, 4, 8,$ and 12 appear in Fig. 10. As the intensity of the external field increases, the break-up is delayed and eventually arrested for large enough Ca_{mag} . Figure 11(a) displays the estimated rupture time, τ_b , as a function of Ca_{mag}^{-1} and clearly indicates that the break-up time increases nonlinearly with the magnetic field intensity. This result also indicates that there is a critical magnetic capillary number Ca_{mag}^* above which rupture does not occur. A power-law fitting suggests that $Ca_{mag}^* \approx 7.15$ and the droplet break-up time scales like $\tau_b \sim (Ca_{mag}^{-1} - Ca_{mag}^{*-1})^{-0.245}$. For $Ca_{mag} > Ca_{mag}^*$, the droplet is so aligned with the flow direction that the shear stress acting on its surface is not strong enough to induce rupture. We also note that for $Ca_{mag} < Ca_{mag}^*$ the size of the satellite droplet relative to the initial droplet size, S_s , decreases with increasing Ca_{mag} , as Fig. 11(b) demonstrates. A power-law fitting yields that the satellite droplet size scales like $S_s \sim (Ca_{mag}^{-1} - Ca_{mag}^{*-1})^{0.359}$. The external field increases the droplet deformation in the flow direction and contributes to its rotation from the extensional to the compressional quadrant of shear. This delays the rupture process and reduces the amount of liquid in the droplet neck, which rips up and gives rise to the satellite droplet. It is worth mentioning that the critical magnetic capillary number Ca_{mag}^* is likely dependent on the dimensionless parameters Re , Ca , λ , and ζ . However, the study of this four-dimensional phase space on the break-up dynamics is a challenging problem and will be addressed in a future work.

A strikingly different behavior takes place when the applied magnetic field is perpendic-

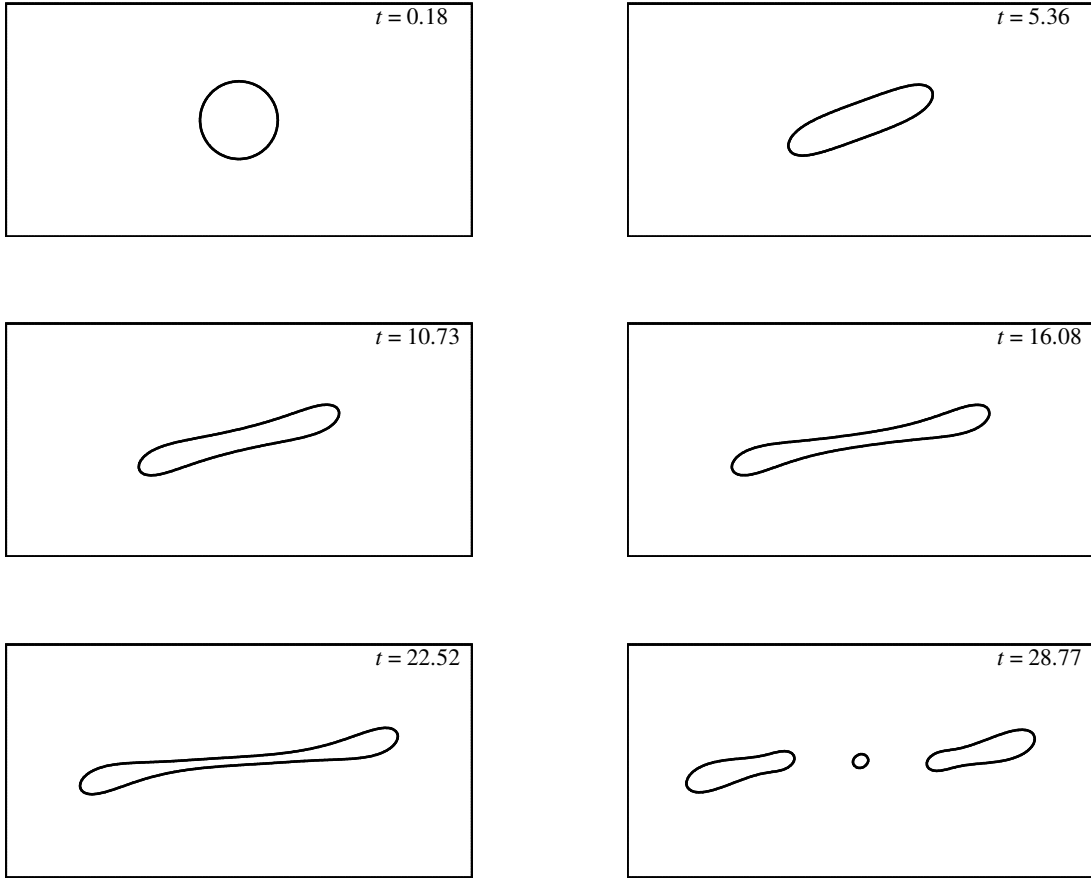


FIG. 9. Evolution of the droplet shape in the absence of an external magnetic field ($Ca_{mag} = 0$). Simulations performed with $Re = 1$, $Ca = 0.5$, $\lambda = 1.2$, and $\zeta = 2$.

ular to the flow direction. Figure 12 shows snapshots of the droplet shape evolution for this case. For instance, at $Ca_{mag} = 2$, the time to rupture and the size of the satellite droplet increase relative to the corresponding values for the case where $Ca_{mag} = 0$, as Fig. 12(a) shows. At an intermediate field intensity, $Ca_{mag} = 4$, the applied field prevents break-up and the droplet attains a stable, steady shape, as Fig. 12(b) displays. Surprisingly, as Ca_{mag} increases, rupture occurs again. The time to break-up decreases and the size of the satellite droplet increases with Ca_{mag} . The droplet evolution for $Ca_{mag} = 8$ and $Ca_{mag} = 12$, when break-up occurs again and in a spectacular form, appears in Figs. 12(c) and 12(d). This complex behavior results from the competition between two distinct effects caused by the perpendicular external field. On the one hand, it deforms the droplet along velocity gradient direction, which increases the shear stress acting on its surface and facilitates an eventual

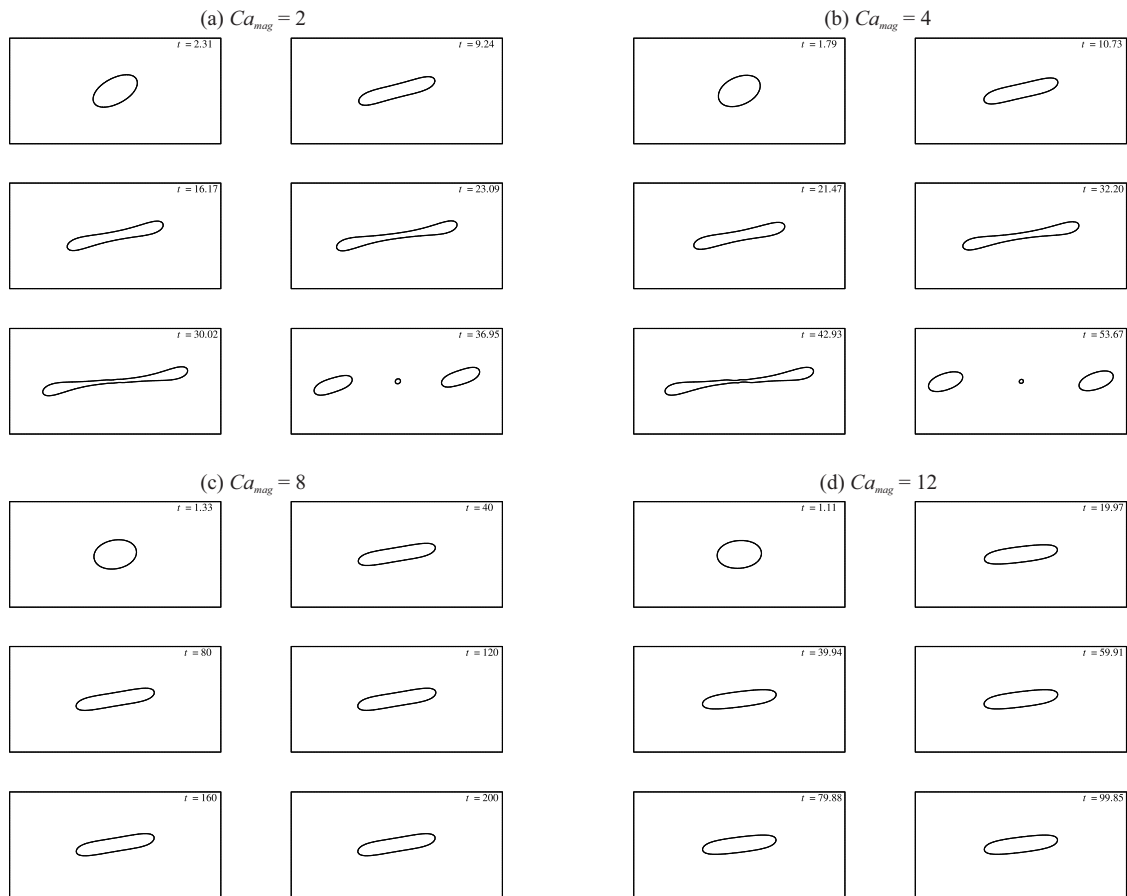


FIG. 10. Evolution of the droplet shape under the action of an external magnetic field parallel to the flow direction for (a) $Ca_{mag} = 2$, (b) $Ca_{mag} = 4$, (c) $Ca_{mag} = 8$, and (d) $Ca_{mag} = 12$. Simulations performed with $Re = 1$, $Ca = 0.5$, $\lambda = 1.2$, and $\zeta = 2$.

break-up. On the other hand, it also makes the droplet neck flatter, which increases the amount of liquid in this region and, as a consequence, hinders the rupture process. Notice that for a high enough field intensity as $Ca_{mag} = 12$, the long satellite droplet undergoes the same process as the initial droplet until it pinches off at the center and gives rise to a secondary rupture.

Finally, we analyze the effect of an external magnetic field on a droplet that does not break-up under the shear action only. To this end, we take $Re = 0.1$, $Ca = 0.3$, $\lambda = 1.2$, and $\zeta = 2$. Again, we consider external fields both parallel and perpendicular to the flow direction, but now we take three different field intensities: $Ca_{mag} = 1$, 10, and 20. For the cases where the external field is parallel to the flow direction, the droplet does not

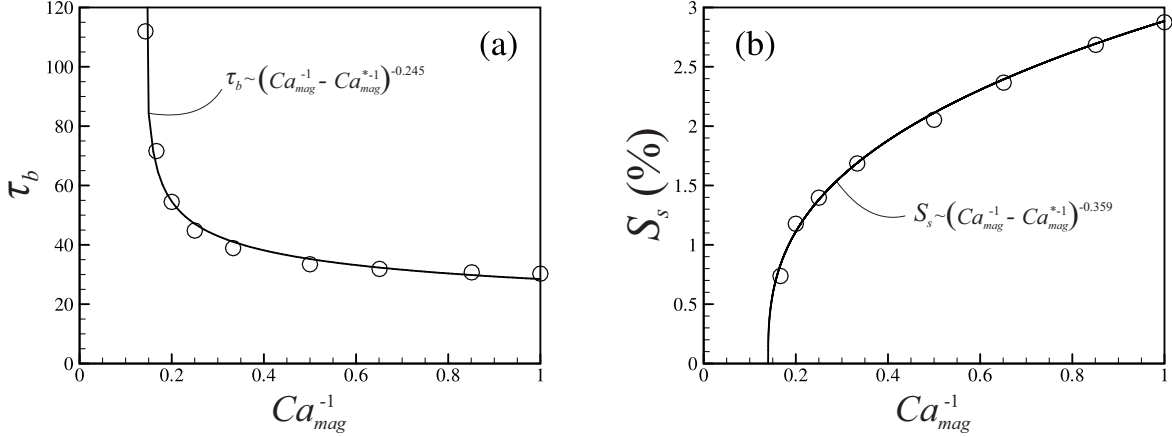


FIG. 11. Effect of an external magnetic field parallel to the flow direction on the break-up of ferrofluid droplets in terms of (a) time to break-up, τ_b , and (b) relative size of the satellite droplet, S_s , as a function of Ca_{mag}^{-1} . Notice that the point corresponding to $Ca_{mag}^{-1} = 1/7$ does not appear in (b) because the size of the satellite droplet in this case is so small that it cannot be measured due to computational limitations.

break and rapidly achieves a stable configuration. Indeed, as discussed so far, for the range of parameters explored here, the field-induced distortion in the flow direction acts as a restorative mechanism of the droplet shape and does not induce rupture. A different result is observed when the external field is perpendicular to the flow direction. At $Ca_{mag} = 1$ and $Ca_{mag} = 10$, the field intensity is not strong enough to induce rupture and the droplet still does not break. However, at $Ca_{mag} = 20$, the field-induced distortion in the velocity gradient direction is so dramatic that the shear stress on the highly elongated droplet is strong enough to induce the break-up. Figure 13 displays the corresponding droplet evolution for this case. Notably, this result indicates that strong enough external magnetic fields perpendicular to the flow direction can be applied to induce droplet break-up in shear flows in which the droplet would not rupture.

V. CONCLUDING REMARKS

We presented a numerical study on the effects of an external, uniform magnetic field on the dynamics and break-up of a two-dimensional supraparamagnetic ferrofluid droplet in simple shear flows. We also explored the role of the external field on the rheology of the

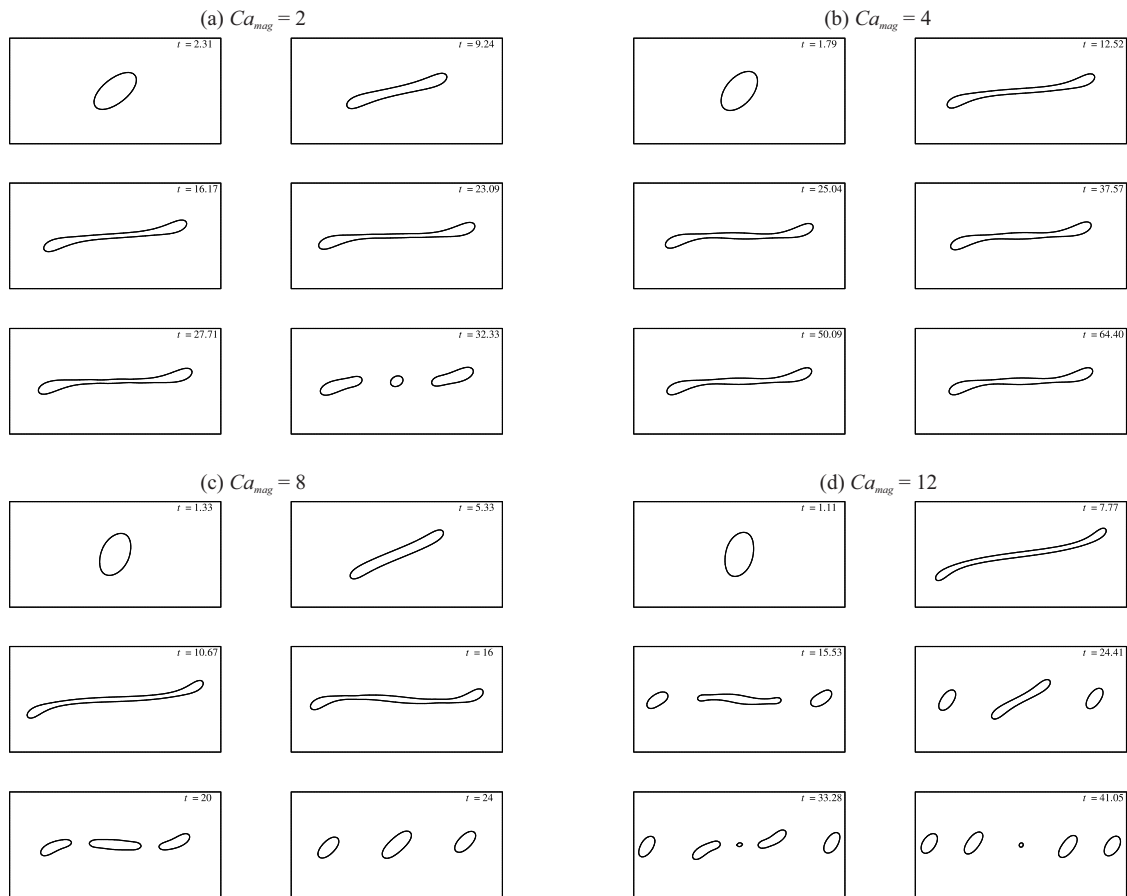


FIG. 12. Evolution of the droplet shape under the action of an external magnetic field perpendicular to the flow direction for (a) $Ca_{mag} = 2$, (b) $Ca_{mag} = 4$, (c) $Ca_{mag} = 8$, and (d) $Ca_{mag} = 12$. Simulations performed with $Re = 1$, $Ca = 0.5$, $\lambda = 1.2$, and $\zeta = 2$.

two-phase fluid system viewed as a model for a dilute emulsion of ferrofluid droplets. The mathematical model consists of the incompressible Navier-Stokes equations, with the added magnetic and capillary forces, coupled with the magnetostatic Maxwell's equations. The dynamics of the droplet surface, including the topological transition during break-up, was captured through the evolution of a level set function.

The results show a clear influence of the applied magnetic field on the droplet deformation and inclination in shear flows, which, in turn, contribute to substantial changes in the emulsion viscosity. When the external field is parallel to the flow direction, the droplet strongly aligns with the flow streamlines, yielding a reduction of the emulsion viscosity. In turn, when the external field is perpendicular to the flow direction, the droplet is forced to

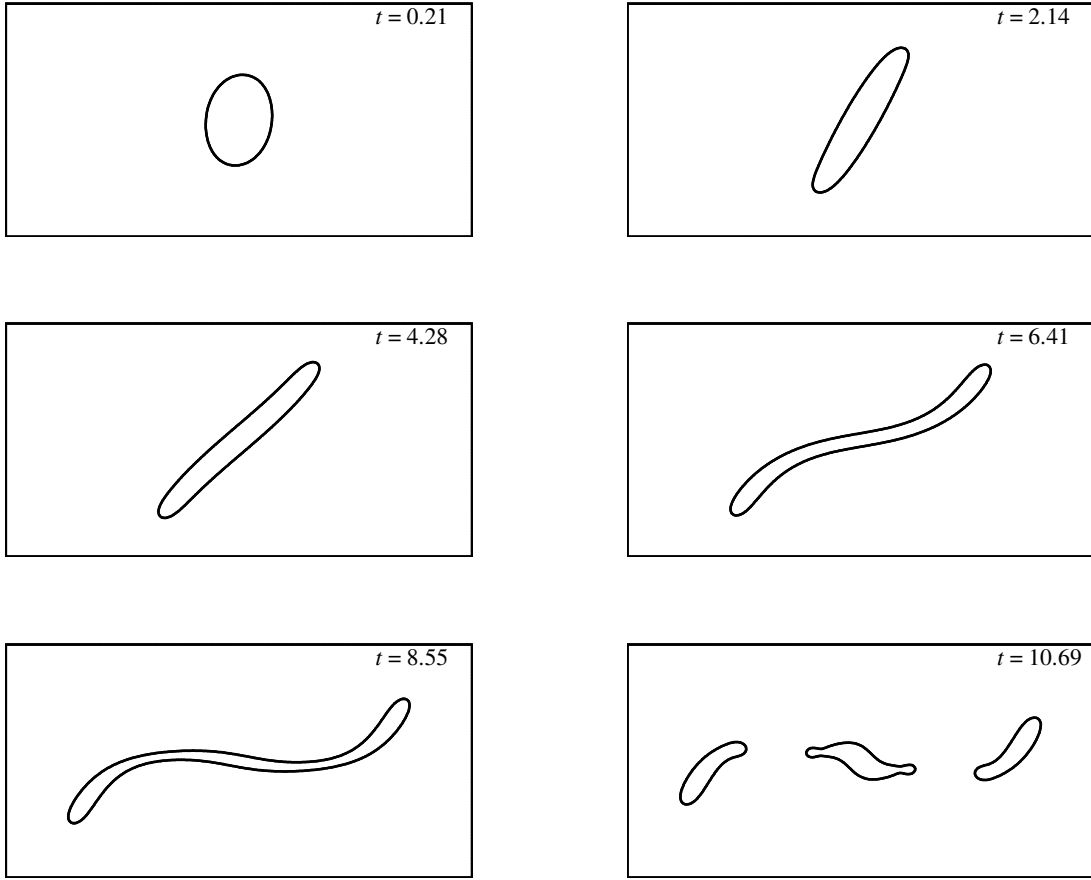


FIG. 13. Evolution of the droplet shape under the action of an external magnetic field perpendicular to the flow direction with $Ca_{mag} = 20$. Simulations performed with $Re = 0.1$, $Ca = 0.3$, $\lambda = 1.2$, and $\zeta = 2$.

align with the field and leads to a large distortion of the flow streamlines. As a result, there is a dramatic increase in the two-phase liquid viscosity.

Our predictions also demonstrate that an external magnetic field can induce or hinder droplet rupture depending on its orientation and intensity (relative to capillary forces). In particular, external fields parallel to the flow direction delay the break-up process and reduce the size of the satellite droplet. Remarkably, it was found that there is a critical magnetic capillary number above which the droplet becomes so aligned with the flow that the break-up process is totally avoided. When the external field is perpendicular to the flow direction, there is a delicate competition between the field-induced stretching in the velocity gradient direction, which facilitates the break-up, and the increase in the amount of liquid in the

droplet neck, which hinders the rupture. This competition leads to a striking result: the intensity of the applied field can be adjusted to either delay, prevent, or induce droplet break-up. Moreover, we also observed that very strong external magnetic fields that are perpendicular to the flow direction can be used to induce droplet break-up in situations where there would be no rupture under the action of the shear flow only.

In summary, the results here presented highlight the enormous potential of external magnetic fields as a tool to control the topology of ferrofluid droplets and the rheology of ferrofluid emulsions.

ACKNOWLEDGMENTS

We would like to acknowledge the financial support from the Brazilian Research Council (CNPq) through the project of number 830015/2005-1. HDC gratefully acknowledges support from the National Science Foundation grant # DMS 1317684.

Appendix A: Mesh convergence test

We present here a mesh convergence test for the overall numerical scheme employed in this work. A representative set of parameters is adopted for this test: $Re = 0.01$, $Ca = 0.1$, $Ca_{mag} = 10$, $\lambda = 2$, $\zeta = 2$ and a 12×12 square domain. The solution was computed up to the time $t = 1.3$ using four different meshes consisting of $N \times N$ cells. The accuracy of the numerical results was assessed by computing the droplet inclination angle, θ , and the emulsion effective viscosity, $[\eta]$. The results are presented in Table I. As can be seen, the four meshes yield very close results. Increasing the number of cells in each direction from $N = 200$ to $N = 400$ changes the effective viscosity in 0.2% and the droplet inclination in 1.6%. This analysis supports the fact that the results presented are independent of the mesh refinement.

REFERENCES

- ¹I. Torres-Díaz and C. Rinaldi, “Recent progress in ferrofluids research: novel applications of magnetically controllable and tunable fluids,” *Soft Matter* **10**, 8584–8602 (2014).

TABLE I. Results for the mesh convergence test.

N	θ	$[\eta]$
100	0.04911	77.1458
200	0.05155	77.6010
300	0.05214	77.7311
400	0.05235	77.7762

- ²R.-J. Yang, H.-H. Hou, Y.-N. Wang, and L.-M. Fu, “Micro-magnetofluidics in microfluidic systems: A review,” *Sensors and Actuators B: Chemical* **224**, 1–15 (2016).
- ³P. Zhu and L. Wang, “Passive and active droplet generation with microfluidics: a review,” *Lab on a Chip* **17**, 34–75 (2017).
- ⁴Q. A. Pankhurst, N. T. K. Thanh, S. K. Jones, and J. Dobson, “Progress in applications of magnetic nanoparticles in biomedicine,” *Journal of Physics D: Applied Physics* **42**, 224001 (2009).
- ⁵I. K. Puri and R. Ganguly, “Particle transport in therapeutic magnetic fields,” *Annual Review of Fluid Mechanics* **46**, 407–440 (2014).
- ⁶Q. Liu, H. Li, and K. Y. Lam, “Optimization of deformable magnetic-sensitive hydrogel-based targeting system in suspension fluid for site-specific drug delivery,” *Molecular Pharmaceutics* **15**, 4632–4642 (2018).
- ⁷J. P. Dailey, J. P. Phillips, C. Li, and J. S. Riffle, “Synthesis of silicone magnetic fluid for use in eye surgery,” *Journal of Magnetism and Magnetic Materials* **194**, 140–148 (1999).
- ⁸P. A. Voltairas, D. I. Fotiadis, and C. V. Massalas, “Elastic stability of silicone ferrofluid internal tamponate (SFIT) in retinal detachment surgery,” *Journal of Magnetism and Magnetic Materials* **225**, 248–255 (2001).
- ⁹O. T. Mefford, R. C. Woodward, J. D. Goff, T. P. Vadala, T. G. S. Pierre, J. P. Dailey, and J. S. Riffle, “Field-induced motion of ferrofluids through immiscible viscous media: Testbed for restorative treatment of retinal detachment,” *Journal of Magnetism and Magnetic Materials* **311**, 347–353 (2007).
- ¹⁰M. Backholm, M. Vuckovac, J. Schreier, M. Latikka, M. Hummel, M. B. Linder, and R. H. A. Ras, “Oscillating ferrofluid droplet microrheology of liquid-immersed sessile droplets,” *Langmuir* **33**, 6300–6306 (2017).

- ¹¹C. K. (Bushueva), K. Kostarev, and A. Shmyrova, “Deformation of ferrofluid floating drop under the action of magnetic field as method of interface tension measurement,” *Experimental Thermal and Fluid Science* **101**, 186–192 (2019).
- ¹²J. D. Sherwood, “Breakup of fluid droplets in electric and magnetic fields,” *Journal of Fluid Mechanics* **188**, 133–146 (1988).
- ¹³O. E. Séro-Guillaume, D. Zouaoui, D. Bernardin, and J. P. Brancher, “The shape of a magnetic liquid drop,” *Journal of Fluid Mechanics* **241**, 215–232 (1992).
- ¹⁴C. Flament, S. Lacis, J.-C. Bacri, A. Cebers, S. Neveu, and R. Perzynski, “Measurements of ferrofluid surface tension in confined geometry,” *Physical Review E* **53**, 4801–4806 (1996).
- ¹⁵S. Banerjee, M. Fasnacht, S. Garoff, and M. Widom, “Elongation of confined ferrofluid droplets under applied fields,” *Physical Review E* **60**, 4272–4279 (1999).
- ¹⁶V. Bashtovoi, S. Pogirnikskaya, and A. Reks, “Dynamics of deformation of magnetic fluid flat drops in a homogeneous longitudinal magnetic field,” *Journal of magnetism and magnetic materials* **201**, 300–302 (1999).
- ¹⁷S. Afkhami, A. J. Tyler, Y. Renardy, M. Renardy, T. G. S. Pierre, R. C. Woodward, and J. S. Riffle, “Deformation of a hydrophobic ferrofluid droplet suspended in a viscous medium under uniform magnetic fields,” *Journal of Fluid Mechanics* **663**, 358–384 (2010).
- ¹⁸P. Rowghanian, C. D. Meinhart, and O. Campàs, “Dynamics of ferrofluid drop deformations under spatially uniform magnetic fields,” *Journal of Fluid Mechanics* **802**, 245–262 (2016).
- ¹⁹S. Afkhami, Y. Renardy, M. Renardy, J. S. Riffle, and T. S. Pierre, “Field-induced motion of ferrofluid droplets through immiscible viscous media,” *Journal of Fluid Mechanics* **610**, 363–380 (2008).
- ²⁰D. Shi, Q. Bi, and R. Zhou, “Numerical simulation of a falling ferrofluid droplet in a uniform magnetic field by the VOSET method,” *Numerical Heat Transfer, Part A: Applications* **66**, 144–164 (2014).
- ²¹D. Shi, Q. Bi, Y. He, and R. Zhou, “Experimental investigation on falling ferrofluid droplets in vertical magnetic fields,” *Experimental Thermal and Fluid Science* **54**, 313–320 (2014).
- ²²J. Liu, Y. F. Yap, and N.-T. Nguyen, “Numerical study of the formation process of ferrofluid droplets,” *Physics of Fluids* **23**, 072008 (2011).

- ²³Y. Wu, T. Fu, Y. Ma, and H. Z. Li, “Active control of ferrofluid droplet breakup dynamics in a microfluidic T-junction,” *Microfluidics and Nanofluidics* **18**, 19–27 (2015).
- ²⁴V. B. Varma, A. Ray, Z. M. Wang, Z. P. Wang, and R. V. Ramanujan, “Droplet merging on a lab-on-a chip platform by uniform magnetic fields,” *Scientific Reports* **6**, 37671 (2016).
- ²⁵H. Li, Y. Wu, X. Wang, C. Zhu, T. Fu, and Y. Ma, “Magnetofluidic control of the breakup of ferrofluid droplets in a microfluidic Y-junction,” *RSC Advances* **6**, 778–785 (2016).
- ²⁶M. Aboutalebi, M. A. Bijarchi, M. B. Shafii, and S. K. Hannani, “Numerical investigation on splitting of ferrofluid microdroplets in T-junctions using an asymmetric magnetic field with proposed correlation,” *Journal of Magnetism and Magnetic Materials* **447**, 139–149 (2018).
- ²⁷C. Flament, G. Pacitto, J.-C. Bacri, I. Drikis, and A. Cebers, “Viscous fingering in a magnetic fluid. I. Radial Hele-Shaw flow,” *Physics of Fluids* **10**, 2464–2472 (1996).
- ²⁸G. Pacitto, C. Flament, and J.-C. Bacri, “Viscous fingering in a magnetic fluid. II. Linear Hele-Shaw flow,” *Physics of Fluids* **13**, 3196–3203 (2001).
- ²⁹J. V. I. Timonen, M. Latikka, L. Leibler, R. H. A. Ras, and O. Ikkala, “Switchable static and dynamic self-assembly of magnetic droplets on superhydrophobic surfaces,” *Science* **341**, 253–257 (2013).
- ³⁰A. Ahmed, B. A. Fleck, and P. R. Waghmare, “Maximum spreading of a ferrofluid droplet under the effect of magnetic field,” *Physics of Fluids* **30**, 077102 (2018).
- ³¹A. Ahmed, A. J. Qureshi, B. A. Fleck, and P. R. Waghmare, “Effects of magnetic field on the spreading dynamics of an impinging ferrofluid droplet,” *Journal of Colloid and Interface Science* **532**, 309–320 (2018).
- ³²W. C. Jesus, A. M. Roma, and H. D. Ceniceros, “Deformation of a sheared magnetic droplet in a viscous fluid,” *Communications in Computational Physics* **24**, 332–355 (2018).
- ³³M. R. Hassan, J. Zhang, and C. Wang, “Deformation of a ferrofluid droplet in simple shear flows under uniform magnetic fields,” *Physics of Fluids* **30** (2018).
- ³⁴P. Capobianchi, M. Lappa, and M. S. N. Oliveira, “Deformation of a ferrofluid droplet in a simple shear flow under the effect of a constant magnetic field,” *Computers & Fluids* **173**, 313–323 (2018).
- ³⁵R. E. Rosensweig, *Ferrohydrodynamics* (Cambridge University Press, 1985).
- ³⁶G. K. Batchelor, “The stress system in a suspension of force-free particles,” *Journal of Fluid Mechanics* **41**, 545–570 (1970).

- ³⁷S. Osher and J. A. Sethian, “Fronts propagating with curvature dependent speed: Algorithms based on Hamilton-Jacobi formulations,” *Journal of Computational Physics* **79**, 12–49 (1988).
- ³⁸G. E. Karniadakis, M. Israeli, and S. A. Orszag, “High-order splitting methods for the incompressible Navier-Stokes equations,” *Journal of Computational Physics* **97**, 414–443 (1991).
- ³⁹V. E. Badalassi, H. D. Ceniceros, and S. Banerjee, “Computation of multiphase systems with phase field models,” *Journal of Computational Physics* **190**, 371–397 (2003).
- ⁴⁰G.-S. Jiang and D. Peng, “Weighted ENO schemes for Hamilton-Jacobi equations,” *SIAM Journal of Scientific Computing* **21**, 2126–2143 (2000).
- ⁴¹C. Min, “On reinitializing level set functions,” *Journal of Computational Physics* **229**, 2764–2772 (2010).
- ⁴²F. Gibou, R. Fedkiw, and S. Osher, “A review of level-set methods and some recent applications,” *Journal of Computational Physics* **353**, 82–109 (2018).
- ⁴³M. Sussman, P. Smereka, and S. Osher, “A level set approach for computing solutions to incompressible two-phase flow,” *Journal of Computational Physics* **114**, 146–159 (1994).
- ⁴⁴G. Ghigliotti, T. Biben, and C. Misbah, “Rheology of a dilute two-dimensional suspension of vesicles,” *Journal of Fluid Mechanics* **653**, 489–518 (2010).
- ⁴⁵H. D. Ceniceros, R. L. N3s, and A. M. Roma, “Three-dimensional, fully adaptive simulations of phase field fluid models,” *Journal of Computational Physics* **229**, 6135–6155 (2010).
- ⁴⁶P. M. Vlahovska, “On the rheology of a dilute emulsion in a uniform electric field,” *Journal of Fluid Mechanics* **670**, 481–503 (2011).
- ⁴⁷S. Mandal and S. Chakraborty, “Effect of uniform electric field on the drop deformation in simple shear flow and emulsion shear rheology,” *Physics of Fluids* **29**, 072109 (2017).
- ⁴⁸S. Mandal and S. Chakraborty, “Uniform electric-field-induced non-Newtonian rheology of a dilute suspension of deformable Newtonian drops,” *Physics Review Fluids* **2**, 093602 (2017).